

# Chemistry A European Journal

 **Chemistry  
Europe**  
European Chemical  
Societies Publishing

## Accepted Article

**Title:** H<sub>2</sub>, B–H, and Si–H bond activation and facile protonolysis driven by Pt–base metal cooperation

**Authors:** Ramadoss Govindarajan, Shubham Deolka, Eugene Khaskin, Robert R. Fayzullin, Shrinwantu Pal, Serhii Vasylevskyi, and Julia Khusnutdinova

This manuscript has been accepted after peer review and appears as an Accepted Article online prior to editing, proofing, and formal publication of the final Version of Record (VoR). The VoR will be published online in Early View as soon as possible and may be different to this Accepted Article as a result of editing. Readers should obtain the VoR from the journal website shown below when it is published to ensure accuracy of information. The authors are responsible for the content of this Accepted Article.

**To be cited as:** *Chem. Eur. J.* **2022**, e202201639

**Link to VoR:** <https://doi.org/10.1002/chem.202201639>

WILEY-VCH

## RESEARCH ARTICLE

# H<sub>2</sub>, B–H, and Si–H bond activation and facile protonolysis driven by Pt–base metal cooperation

Ramadoss Govindarajan,<sup>[a]</sup> Shubham Deolka,<sup>[a]</sup> Eugene Khaskin,<sup>[a]</sup> Robert R. Fayzullin,<sup>[b]</sup> Shrinwantu Pal,<sup>[a]</sup> Serhii Vasylevskyi,<sup>[a]</sup> and Julia R. Khusnutdinova\*<sup>[a]</sup>

[a] Dr. R. Govindarajan, S. Deolka, Dr. E. Khaskin, Dr. S. Pal, Dr. Vasylevskyi, Prof. J. R. Khusnutdinova  
Coordination Chemistry and Catalysis Unit  
Okinawa Institute of Science and Technology Graduate University  
1919-1 Tancha, Onna-son, Okinawa, Japan 904-0495  
E-mail: juliak@oist.jp

[b] Dr. Robert R. Fayzullin  
Arbuzov Institute of Organic and Physical Chemistry  
FRC Kazan Scientific Center, Russian Academy of Sciences  
8 Arbuzov Street, Kazan, 420088, Russian Federation

Supporting information for this article is given via a link at the end of the document.

**Abstract:** We report a series of heterobimetallic Pt/Zn and Pt/Ca complexes to study the effect of proximity of a dicationic base metal on the organometallic Pt species. Varying degrees of Pt···Zn and Zn interaction with the bridging Me group are achieved, showcasing snapshots of a hypothetical process of retrotransmetalation from Pt to Zn. In contrast, only weak interactions were observed for Ca with a Pt-bound Me group. Activation of H<sub>2</sub>, B–H and Si–H bonds leads to the formation of hydride-bridged Pt–H–Zn complexes, which is not observed in the absence of Zn, pointing out the importance of metal-metal cooperation. Reactivity of PtMe<sub>2</sub>/M<sup>2+</sup> with terminal acetylene, water and methanol is also studied, leading to facile protonation of one of the Me group at the Pt center only when Zn is present. This study sheds light at various ways in which the presence of a 2+ metal cation significantly affects the reactivity of a common organoplatinum complex.

## Introduction

The use of base metal additives to control the activity and selectivity of the noble metal catalyst has widespread applications both in homogeneous and heterogeneous catalysis.<sup>[1]</sup> However, the effect of the base metal additive on the reactivity of the noble metal center is often poorly understood due to lack of well-defined models to elucidate how the presence of the second metal cation affects the reactivity of the catalytically active site. In homogeneous catalysis, the most well-known example of metal-metal cooperativity is Pd/Cu-catalyzed C–C coupling reactions, such as Sonogashira coupling, in which Cu participates in the transmetalation step to Pd.<sup>[2]</sup> To this end, several heteromultimetallic compounds aimed to model an interaction between the organometallic Pd center and Cu have been reported.<sup>[3] [4]</sup> At the same time, the effect of other base metal additives, in particular dicationic ions such as Zn, Mg etc, which are also often used in cross-coupling reactions, has not been studied to the same degree.<sup>[5]</sup> For example, Pd···Zn interactions have been proposed to play an important role in Negishi cross-coupling, particularly in the transmetalation and retrotransmetalation steps, the latter leading to undesired homocoupling products.<sup>[6]</sup> Tilley and co-workers reported

significantly accelerated rate of aryl-aryl reductive elimination from Pt<sup>II</sup> complexes showing interactions with bis(perfluorophenyl)zinc or aryl group exchange between Pt and Zn, depending on the nature of the ligand.<sup>[7]</sup> Recently, the ability of coordinated ZnMe to promote facile H<sub>2</sub> activation in Ru/Zn heterobimetallic complexes has been demonstrated by Miloserdov, Macgregor and Whittlesey.<sup>[8]</sup> However, in the case of H<sub>2</sub> activation by a Ru/ZnEt complex, Ru plays a key role and the DFT calculations suggest that H<sub>2</sub> activation via oxidative cleavage at Ru would similarly occur even if the Zn atom is unable to accept a hydride.<sup>[8b]</sup> Interestingly, utilization of Zn to enhance reactivity and selectivity of a Pt center also gained attention in heterogeneous catalysis. For example, precise design of Pt/Zn intermetallic nanoparticles has been shown to affect selectivity of a Pt center in hydrogenation, and Zn/Pt and Zn/Pd intermetallic compounds have been reported as catalysts for light alkane dehydrogenation.<sup>[9]</sup> However, because of the intrinsic complexity of heterogeneous systems, the synergistic effect of the presence of both Pt and Zn centers in bond activation lacks precise understanding.

We have previously described our strategy to bring two metal centers into close proximity with each other by using a soft/hard donor binucleating ligands.<sup>[10]</sup> This strategy was used to study Pt<sup>I</sup>/Cu<sup>I</sup> and Pd<sup>II</sup>/Cu<sup>I</sup> interactions on the reactivity in transmetalation, cyclometallation, and terminal alkyne C–H bond activation. The presence of Pt···Cu interactions was found to have a crucial effect on the reactivity of the Pt center, either acting as a substrate docking site (at the Cu center) leading to the polarization of the C–H bond, or by stabilizing the bimetallic assembly through metal-metal bonding, which was studied in detail through QTAIM and NBO analyses.<sup>[10a]</sup>

As part of an effort to examine less studied and more challenging systems, we focused on an organometallic Pt center in proximity with another d<sup>10</sup> metal, Zn, which is generally less studied in forming bonding interaction with Pt group metals,<sup>[11]</sup> as well as Ca, which has not been previously studied in the context of heterobimetallic interactions with organoplatinum complexes. Herein we report selective formation of organometallic Pt/Zn and Pt/Ca compounds and their metal-metal cooperative reactivity, leading to activation of H<sub>2</sub>, B–H, Si–H bonds, C–H bonds in terminal alkyne, as well as Zn-promoted mild protonolysis by

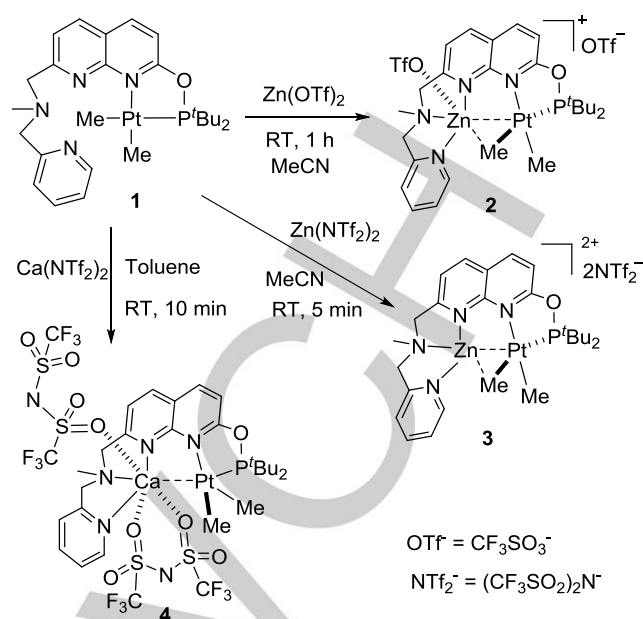
## RESEARCH ARTICLE

small amounts of water and methanol. Notably, activation of H<sub>2</sub>, boranes and silanes leading to bridging Pt–H···Zn complexes does not occur at mononuclear Pt complex in the presence of a Zn salt additive, highlighting the importance of metal-metal proximity in bond activation, with the second metal directly participating in product stabilization. This substrate activation mode is fundamentally different from traditionally reported frustrated Lewis pair (FLP)-type reactivity in metal-only Lewis pairs,<sup>[12]</sup> or when base metals are used simply as Lewis acid additives.<sup>[13]</sup> We also discuss how varying the coordination environment around Zn leads to changes in the interaction of the bridging Me group with Zn, resembling the earlier proposed retrotransmetalation from Pd to Zn, which is assumed to occur in Negishi coupling in which Pt group metal···Zn interactions play an important role.

## Results and Discussion

**Synthesis of heterobimetallic complexes.** We utilized a previously developed binucleating ligand bearing soft and hard donor sites tethered to a binucleating naphthyridine fragment.<sup>[10a]</sup> First, a mononuclear Pt dimethyl complex **1** was synthesized as described previously,<sup>[10a]</sup> followed by a second metalation step with zinc triflate, zinc bistriflimide or calcium bistriflimide to yield complexes **2**, **3** and **4**, respectively (Scheme 1). Attempted metalation with calcium triflate led to the mixture of unidentified products. Similarly attempted reaction of **1** with Mg triflate or bistriflimide did not afford any stable isolated heterobimetallic complexes.

Complexes **2** and **3** were isolated in 92% and 86% yields respectively, and characterized by multinuclear NMR, IR, UV/vis spectroscopy, electrospray ionization, high resolution mass spectrometry (ESI-HRMS), and single crystal X-ray diffraction (SC-XRD) (Figure 1a,b). The ESI-HRMS spectrum of complex **2** shows a monocationic mass envelope with the expected isotopic pattern corresponding to a simulated spectrum (Figure S7). Similarly, complex **3** also shows the expected mass envelope in ESI-HRMS as an adduct with one triflimide (Figure S16). The formation of complex **4** was monitored by NMR spectroscopy in solution which showed complete conversion in toluene or benzene leading to characteristic changes in the NMR spectra. In particular, coordination of Ca atom at the picolylamine terminus is indicated by the appearance of four doublets from two geminally coupled CH<sub>2</sub> groups that become non-equivalent upon coordination to the metal. In addition, the <sup>31</sup>P and <sup>195</sup>Pt signals are shifted upon Ca coordination from  $\delta_P$  183.9 ppm and  $\delta_{Pt}$  –3894 (<sup>1</sup>J<sub>PtP</sub> = 2006 Hz) in complex **1** to  $\delta_P$  184.7 ppm and  $\delta_{Pt}$  –3987 (<sup>1</sup>J<sub>PtP</sub> = 2262 Hz) in complex **4**. Formation of **4** in solution was also confirmed by ESI-HRMS showing the expected isotopic pattern (Figure S25). Complex **4** could be crystallized and characterized by SC-XRD (Figure 1c), but was unstable in the presence of polar coordinating solvents or when dried under vacuum.



Scheme 1. Synthesis of **2**, **3** and **4**.

Interestingly, comparing of X-ray structures of **2** and **3** revealed significant differences in the metal-carbon bond lengths of the Me group proximal to Zn atom (Table 1). In the monocationic **2**, Zn is coordinated to O-atom of one of the triflate anions, with the Zn···C1 distance being relatively long, 2.388(4) Å, while the Pt–C1 bond length is 2.132(3) Å. In contrast, in the dicationic complex **3**, where Zn does not have coordinating interactions with the anion, the corresponding Zn···C1 distance of 2.157(7) Å is significantly shorter. For comparison, the Zn–C distance in Zn mono- and dimethyl complexes with N-donor ligands is typically 1.975–2.008 Å and the Zn–C bond distance in dimethyl zinc ( $\alpha$ -ZnMe<sub>2</sub> phase) is 1.927(6) Å.<sup>[14]</sup> The shortening of the Zn–C distance is accompanied by an elongation of the Pt–C1 bond in **3** (2.247(5) Å) as compared to **2**. While the metal-carbon bond distances change significantly depending on anion coordination, the Pt···Zn distances are only slightly different, 2.6138(4) and 2.6567(7) Å in complexes **2** and **3**, respectively, which is significantly shorter than the sum of the metals' van der Waals radii (3.1–4.2 Å) and slightly longer than the sum of their covalent radii (2.58 Å).<sup>[15]</sup> Therefore, the major differences between **2** and **3** are in the degree of interaction of Zn<sup>2+</sup> with the proximal Me group, leading to much shorter Zn–C bond distance in the absence of coordinated OTf. This is also consistent with the computational analysis (vide infra) showing that Me group essentially plays a role of the bridging ligand shared between Pt and Zn atoms via a three-center two-electron (3c2e) bonding.<sup>[10a, 16]</sup> This resembles DFT-computed structures and binding modes in the intermediates and transition states for the retrotransmetalation from Pd to Zn and Zn-catalyzed isomerization of Pd intermediates relevant to Negishi cross-coupling reported by Espinet, Álvarez, Casares, et al.<sup>[6, 17]</sup> In particular retrotransmetalation from Pd to Zn as well as a Zn interaction with Pd complexes are proposed to be involved in undesired side-reactivity and homocoupling product formation in Negishi cross-coupling.<sup>[18]</sup> Although complexes reported in this work contain Pt and not Pd, platinum complexes have been widely used to experimentally model transmetalation step relevant to Pd catalysis.<sup>[19]</sup> Similar to our experimentally obtained structures, the computer models also predicted 3c2e bonding of the bridging Me

## RESEARCH ARTICLE

group and the presence of Pd $\cdots$ Zn interactions in the intermediates and transition states along the reaction pathway. Therefore, complexes **2** and **3** can be seen as snapshots of the retrotransmetalation showing that greater degree of Me group binding to Zn is achieved in less coordinatively saturated, 2+ charged Zn center.

Comparison between Pt/Zn and Pt/Ca complexes shows that the Pt–C1 bond length (2.126(3) Å) in complex **4** is only slightly shorter than the analogous Pt–C1 bond in **2**. The Ca $\cdots$ C1 distance for the main component is 2.895(5) Å (Table 1). For comparison, the Ca–C distances in Ca–Me complexes vary from 2.592–2.673 Å for  $\mu^2$ -bridging Me group and 2.477–2.507 Å for terminal Ca–Me.<sup>[20]</sup> Interestingly, the Pt $\cdots$ Ca distance (3.034(9) Å) is shorter than the sum of covalent (3.12 Å) radii, suggesting that weak interactions might also be present, which was further analyzed computationally (vide infra). Analysis of the reported structures showing relatively close interactions between Pt and Ca centers (within 4 Å or less) shows only three lantern-type, non-organometallic Pt/Ca complexes with Pt $\cdots$ Ca distances of 3.064, 2.960 and 3.245 Å.<sup>[21]</sup> Therefore, complex **4** is a rare example of the organometallic Pt/Ca complex with close intermetallic distances.

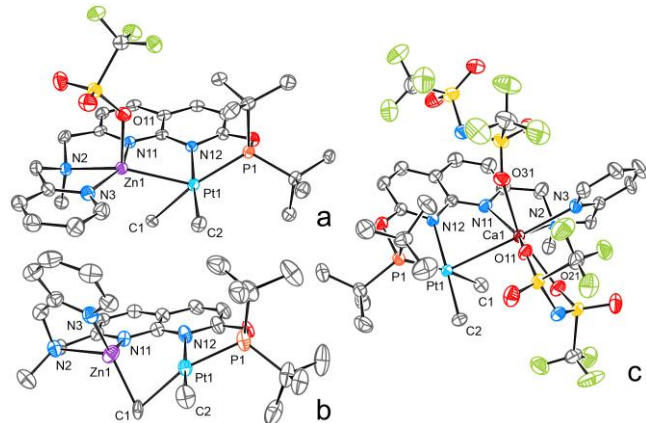


**Figure 1.** Structures of **2** (a), **3** (b), and **4** (c) in the crystals with thermal ellipsoids at the 50 % (a, b) or 60 % (c) probability level. All hydrogen atoms, co-crystallized molecules, non-coordinated counterions, and minor disorder components are omitted for clarity.<sup>[22]</sup>

**Table 1.** Selected interatomic distances in complexes **2–4** determined by SC-XRD.

Interatomic distance	<b>2</b> (M = Zn)	<b>3</b> (M = Zn)	<b>4</b> <sup>[a]</sup> (M = Ca)
Pt–C1	2.132(3)	2.247(5)	2.126(3)
Pt–C2	2.052(3)	2.056(6)	2.048(2)
M–C1	2.388(4)	2.157(7)	2.895(5)/ 2.735(10)
Pt–M	2.6138(4)	2.6567(7)	3.034(4)/ 3.034(9)

[a] Values for the major and minor disorder components are given through a slash.

### Activation of H<sub>2</sub>, B–H, and Si–H bonds.

Considering that the reactivity of noble metal complexes in homogeneous hydrogenation may be enhanced in the presence of Lewis acid additives,<sup>[13, 23]</sup> we set out to investigate whether the

presence of Zn center in proximity to Pt enhances formation of metal hydrides by activation of H<sub>2</sub> and common hydride sources. First, **2** was exposed to 5 bar of H<sub>2</sub> gas in dichloromethane. While only a slow reaction was observed at RT, upon mild heating at 45 °C, a clean transformation occurred, accompanied by the appearance of a Pt hydride signal at –1.67 ppm (<sup>1</sup>J<sub>HPt</sub> = 893.0 Hz and <sup>2</sup>J<sub>HPt</sub> = 131.6 Hz) and elimination of CH<sub>4</sub> (Scheme 2 and Figure S36). The reaction was complete after 72 h, and the product was isolated in 90% yield and characterized by NMR, UV/vis, IR spectroscopy, ESI-HRMS and SC-XRD. ESI-HRMS confirmed the presence of the expected cationic fragment with a good match between experimental and simulated spectra (Figure S34). Accordingly, when the reaction was performed under 5 bar of D<sub>2</sub>, CH<sub>3</sub>D was detected by <sup>1</sup>H NMR at 0.19 ppm (<sup>2</sup>J<sub>HD</sub> = 2.05 Hz), while the <sup>31</sup>P signal also showed characteristic D splitting (<sup>2</sup>J<sub>PD</sub> = 19.4) (Figures S37–S38). <sup>2</sup>H NMR indicated the presence of a Pt–D peak at –1.63 ppm (d, <sup>2</sup>J<sub>PD</sub> = 20.0 Hz, <sup>1</sup>J<sub>PtD</sub> = 137.23 Hz) (Figure S39).

The X-ray structure of hydride complex **5** shows formation of a bimetallic Pt/Zn complex with bridging hydride (Figure 2a), while Zn remains coordinated to three N-atoms and one O-atom of triflate. The Pt $\cdots$ Zn distance in **5** (2.7102(7) Å) is significantly longer compared to **2**, suggesting that no metal-metal interactions are present.

The same hydride complex **5** could be obtained cleanly using common hydride sources. Treating **2** with 2 equiv. of pinacolborane at 45 °C gave **5** in 85% yield after 72 h, accompanied by the formation of methylboronic acid pinacol ester that was detected by GC-MS and <sup>11</sup>B NMR (Figures S40–S41). Similarly, **2** reacted with 2 equiv. of phenylsilane for 18 h at RT resulting in clean formation of **5**, isolated in 84% yield. The formation of methylphenylsilane was detected by GC-MS (Figure S44).

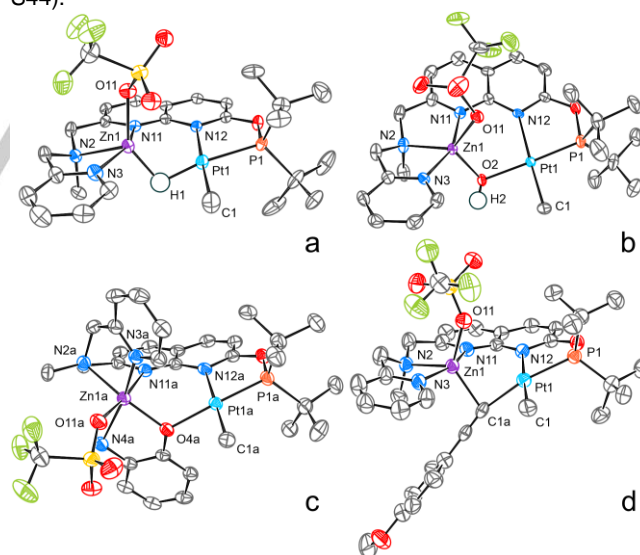
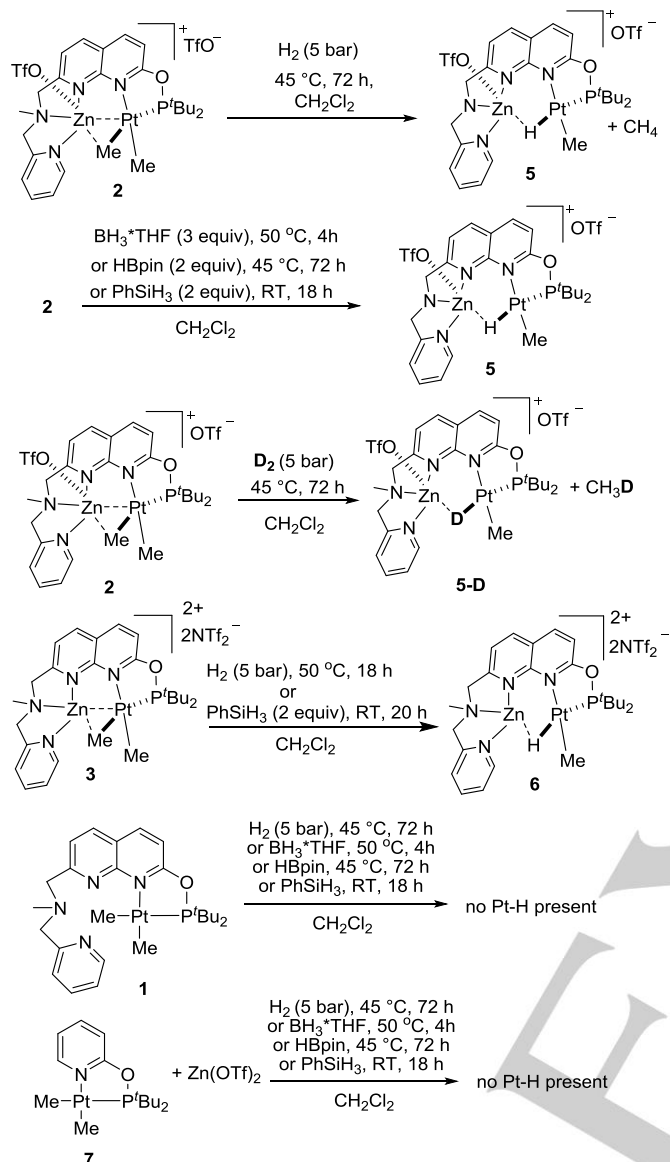


**Figure 2.** Crystal structures of **5** (a), **8** (b), **10** (c), and **11** (d) with thermal ellipsoids at the 50 % (a, c, d) or 60 % (b) probability level. All hydrogen atoms except for [O,Pt]H, co-crystallized molecules, non-coordinated counterions, and minor disorder components are omitted for clarity. In the case of **10**, only one of two symmetrically independent molecules is shown.<sup>[22]</sup>

## RESEARCH ARTICLE



**Scheme 2.** Reactivity of **1**, **2**, **3** and **7** with H<sub>2</sub>, D<sub>2</sub>, pinacolborane and PhSiH<sub>3</sub>.

Similarly, when complex **3** was exposed to 5 bar of H<sub>2</sub> gas at 50 °C for 18 h or 2 equiv. of phenylsilane at RT for 20 h, complex **6** formed, which was isolated in 76% and 64% yields, respectively, and characterized by NMR and SC XRD (see Supporting Information for details). Pt-bound hydride signal appeared at –1.74 ppm in <sup>1</sup>H NMR (<sup>1</sup>J<sub>HPt</sub> = 883.1 Hz and <sup>2</sup>J<sub>HPt</sub> = 127.3 Hz) (Scheme 2 and Figure S53), similar to the analogous Pt-H signal in complex **5**.

To establish whether the presence of Zn had an effect on the hydride formation, we compared the reactivity of **2** with a simple mononuclear Pt-only complex **1**. When **1** was treated with H<sub>2</sub>, PhSiH<sub>3</sub> or pinacolborane, no Pt-H signal was observed, and prolonged reaction time led to decomposition, suggesting that the presence of Zn in the heterobimetallic complex **2** was important to promote metal hydride formation and/or stabilize the product. To examine whether the close proximity between Pt and Zn as enforced by our binucleating ligand was a determining factor in the observed metal-metal cooperative reactivity, we further examined the reactivity of a mononuclear Pt dimethyl complex (**7**) with a simple model ligand, (di-*tert*-butylphosphinito)pyridine, in the presence of Zn(OTf)<sub>2</sub> as an additive. Complex **7** was treated

with H<sub>2</sub>, pinacolborane and PhSiH<sub>3</sub> in the presence of equivalent amount of Zn(OTf)<sub>2</sub> under conditions used for studying complex **2** reactivity, however, no discernible Pt-H signals could be observed in the expected region (0 to –30 ppm) and according to <sup>31</sup>P{<sup>1</sup>H} NMR, a complex mixture of products formed after prolonged reaction time. This confirms that the proximity of Zn to the Pt center in a heterobimetallic complex is the crucial factor determining facile and selective activation of H–H, B–H and Si–H bonds. Our result with Pt<sup>II</sup> can be contrasted to previous reports wherein the reactivity of a Pt(0) complex in H<sub>2</sub> activation was enhanced by additives of Zn(OTf)<sub>2</sub> via frustrated Lewis pair (FLP) type behavior.<sup>[12]</sup>

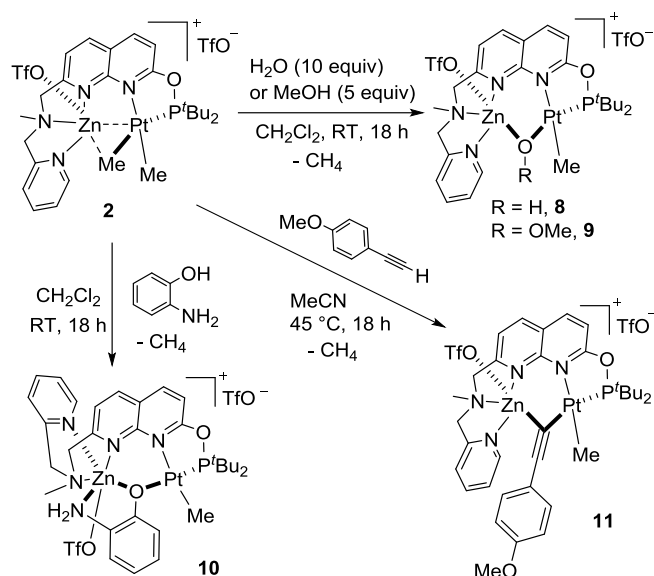
When complex **4** was treated with H<sub>2</sub>, silanes or boranes under analogous conditions, no clearly identified Pt-H signal could be observed, and eventually a mixture of unidentified products was obtained, likely due to the low stability of **4**.

**Protonolysis by water and alcohols and reactivity with terminal alkynes.** Considering that facile hydrogenolysis occurs in Pt/Zn complex **2**, we anticipated that the presence of Zn will also facilitate mild and selective protonolysis of one of the Pt–Me groups using neutral protic solvents, or even acidic C–H bonds. Indeed, when only 10 equiv. of water were added to the dichloromethane solution of **2**, a new monomethyl complex **8** formed cleanly, isolated in 91% yield (Scheme 3). When the reaction was monitored by NMR in CD<sub>2</sub>Cl<sub>2</sub> solution, a peak of methane was clearly observed (Figure S83). Similarly, **2** also reacted with 5 equiv. of CH<sub>3</sub>OH to give **9**. The analogous reaction with CD<sub>3</sub>OD followed by NMR showed a characteristic peak of CH<sub>3</sub>D at 0.19 ppm (<sup>2</sup>J<sub>HD</sub> = 1.6 Hz) (Figure S96).

Both complexes were isolated and characterized by NMR, UV/vis, IR spectroscopy, and ESI-HRMS. The X-ray structure of complex **8** shows that a monomethyl Pt center is present containing an OH group bridging between Pt and Zn atoms (Figure 2b). Although the crystal structure of **9** was not obtained, HRMS analysis of both **8** and **9** was consistent with the presence of the monocationic monomethyl Pt/Zn hydroxide and methoxide complexes respectively (Figures S80 and S95). Based on this, we expect that complex **9** is a methoxide-bridged complex, with a MeO peak observed at 3.46 ppm in <sup>1</sup>H NMR spectrum. This was also confirmed by a nuclear Overhauser effect (NOE) NMR experiment (Figure S92).

As expected, complex **2** also reacted with the more acidic 2-aminophenol, forming complex **10** as characterized spectroscopically and by ESI-HRMS. The SC-XRD structure of **10** shows a phenolate O-donor bridge between Pt and Zn centers with an amine donor bound to Zn (Figure 2c). XRD structures of both complexes **8** and **10** feature significantly elongated Pt···Zn distances (3.2092(7) in **8** and 3.4574(5) and 3.4560(5) Å in the two symmetrically independent molecules **10** in the crystal), indicative of negligible heterobimetallic interactions in these complexes. The presence of such long intermetallic distances also shows that the presence of naphthyridine fragment bridging between two metals does not necessarily impose short intermetallic distances and a great degree of variability in metal-metal distances can be achieved depending on coordination environment and the presence or absence of stabilizing metal-metal interactions. In turn, these results also suggest that once the Zn coordination sphere is supplemented by the coordination to conventional O- or N-donor ligands such as those in **8** and **10**, Pt···Zn interactions are essentially absent in these complexes.

## RESEARCH ARTICLE



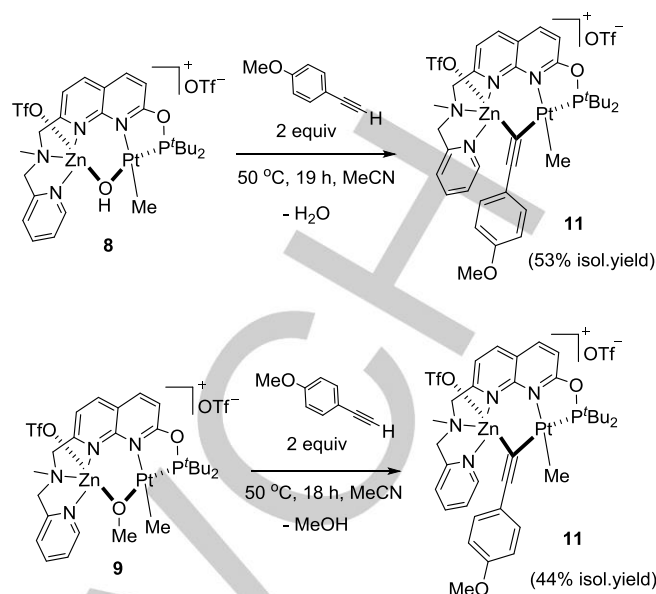
**Scheme 3.** Protonolysis of **2** with water, methanol, and aminophenol and reactivity with 4-ethynylanisole.

The facile protonolysis of Pt-Me group even by water and methanol is likely due to the presence of the Lewis acidic Zn center in close proximity to Pt, which may coordinate protic solvents increasing their acidity.<sup>[24]</sup> By comparison, mononuclear Pt-only complex **1** showed no reactivity with MeOH under analogous conditions and only minor decomposition in the presence of water.

We next examined the reactivity of **2** with 4-ethynylanisole. While the reaction was slow at RT, mild heating at  $45^\circ\text{C}$  for 18 h resulted in the formation of acetylide-bridged complex **11** isolated in 53% yield, accompanied by the loss of one Me group at Pt. This reactivity is analogous to our previously reported metal-metal cooperative activation of alkyne in Cu...Pt complex leading to an analogous acetylide-bridged product.<sup>[10a]</sup> Consistent with our previous reports, no reactivity was observed under analogous conditions in the absence of Cu or Zn, in the Pt-only complex **1**.<sup>[10a]</sup> This result shows that the selective and clean formation of Pt monoacetylide requires the presence of the Lewis acidic activator, which further stabilizes the product through bridging coordination of acetylide ligand between two metals.

Considering that terminal alkynes contain relatively acidic C-H bonds, we decided to explore the potential of using hydroxide or methoxide bridged complexes **8** and **9** to promote deprotonation of a terminal alkyne (Scheme 4).<sup>[25]</sup> Indeed, the reaction of both **8** and **9** resulted in the formation of the same acetylide-bridged complex **11** as confirmed by NMR spectroscopy. This shows that even bridging hydroxide and alkoxide ligands, that may be more likely to form under catalytic conditions than Me bridged **2-4** were highly reactive in acidic C-H bond deprotonation; we plan to further explore this reactivity in metal-metal cooperative functionalization of reactive C-H bonds.

Overall, this reactivity comparison clearly demonstrates that the presence of Zn in close proximity to Pt alters the latter's reactivity by promoting  $\text{H}_2$ , Si-H and B-H bond activation as well as mild and selective protonolysis of only one Pt-Me group even in the presence of small excess of weakly acidic proton sources, including water, alcohols and terminal alkynes.



**Scheme 4.** Reactivity of **8** and **9** with terminal acetylene.

#### Analysis of metal-ligand and metal-metal interactions by QTAIM and NBO.

To analyze metal-metal and metal-ligand binding in Pt/Zn and Pt/Ca heterobimetallic complexes, we performed computational analysis for the DFT-optimized structures of complexes **2-6** and **11** within the Quantum Theory of Atoms in Molecules (QTAIM)<sup>[26]</sup> and Natural Bond Orbital (NBO) analysis.<sup>[27]</sup>

Atoms in Molecules (AIM) analysis for complex **2** reveals a bond critical point (bcp) located between Pt and Zn atoms (Figure 3a) with characteristics similar for closed-shell, metal-metal interactions and resembling bonding between Pt and Cu supported by the same ligand framework reported by us earlier. In contrast, complex **3** did not exhibit bcp directly between Pt and Zn atoms, however, a bcp was present between the carbon of the proximal Me group and Zn, which was absent in **2** (Figure 3b). This is consistent with much shorter Zn-C distances in the proximal Me group in **3** compared to **2** in experimental X-ray structures. For comparison, complex **4** shows only weak, almost negligible interactions between Ca and Pt characterized by relatively low electron density at the bcp (0.021 a.u. vs. 0.048 a.u. in **2**).

The binding mode was further elucidated by NBO analysis and comparison of Natural Binding Indices (NBI) in these complexes (Table 2). Consistent with AIM analysis, the natural binding index (NBI) between Pt and carbon atom of the bridging Me group in **3** is decreased compared to **2**, while the NBI between Zn and the same bridging carbon is increased, indicative of redistribution of electron density along Pt-Me-Zn binding motif. At the same time, the NBI between Pt and the distal (Zn non-interacting) Me group remains almost unchanged in all complexes with almost the same value as in Zn-free complex **1** (0.83).<sup>[10a]</sup>

The binding between bridging Me group and Zn in complex **3** can be described as the donation from the  $\text{C}(sp^3)$  carbon of the bridging Me group to an  $s$ -type Zn orbital, characterized by second order perturbation energy,  $E^{(2)}$ , of  $25.15 \text{ kcal mol}^{-1}$ . In complex **2**, proximal Pt-Me group interaction with Zn is described as the donation from the  $\sigma$ -bonding Pt-Me orbital ( $\sigma\text{-Pt-C}(sp^3)$ ) to the  $s$ -orbital on Zn ( $E^{(2)}$   $162.79 \text{ kcal mol}^{-1}$ ). For comparison, the analogous  $\sigma\text{-Pt-C}(sp^3)$  to Ca( $s$ ) donation is much weaker ( $E^{(2)} = 29.24 \text{ kcal mol}^{-1}$ ) in complex **4**. The previously reported Pt/Cu

## RESEARCH ARTICLE

complex features a similar donation from the proximal  $\sigma$ -Pt-C( $sp^3$ ) to an empty Cu-based  $s$ -type orbital characterized by  $E^{(2)}$  of 89.68 kcal mol $^{-1}$ .<sup>[10a]</sup>

Overall, these results suggest that bridging Me group participates in  $3c2e$  bonding between Pt and Zn, with the degree of Pt–C, Pt–Zn and Zn–C binding controlled by the charge and coordination environment at Zn atom, while its interaction with Ca in **4** is negligibly weak.

Different extent of Pt...Zn metallophilic interactions in **2** and **3** is also consistent with natural bond orbital analysis showing considerably strong donation from the Pt-based  $d$ -orbital to the  $s$ -orbital on Zn in **2** (characterized by second order perturbation energy,  $E^{(2)}$ , of 77.59 kcal mol $^{-1}$ ) as compared to moderate Pt( $d$ )  $\rightarrow$  Zn( $s$ ) donation in **3** ( $E^{(2)}$  = 39.06 kcal mol $^{-1}$ ). Even weaker donation from the Pt-based  $d$ -orbital to the  $s$ -orbital on Ca ( $E^{(2)}$  = 25.26 kcal mol $^{-1}$ ) in **4** suggests only minor contribution of heterobimetallic interactions between Pt and Ca.

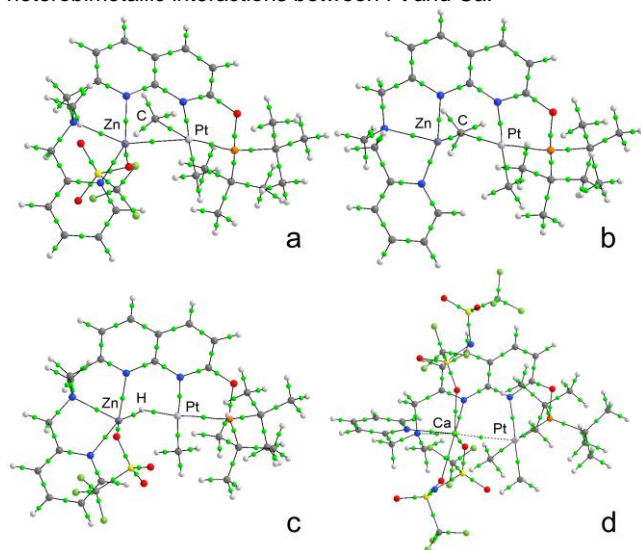


**Figure 3.** Molecular graphs for “gas-phase” DFT-optimized complexes **2** (a), **3** (b), **4** (c), **5** (d) and **11** (e). Bond critical points with a threshold of electron density above 0.025 a.u. and corresponding bond paths are shown with green dots and black lines, respectively. As the electron density between Pt and Ca (0.021 a.u.) was below the threshold for weak critical point (0.025 a.u.), the corresponding bond path is shown in dashed line.

**Table 2.** Selected Natural Binding Indices (NBI) in complexes **2–4**.<sup>[a]</sup>

Binding atoms	<b>2</b> (M = Zn)	<b>3</b> (M = Zn)	<b>4</b> (M = Ca)
NBI (Pt–M)	0.331	0.313	0.223
NBI(Pt–C) (proximal)	0.693	0.563	0.725
NBI(M–C) (proximal)	0.318	0.492	0.146
NBI(Pt–C) (distal)	0.832	0.839	0.837

[a] For gas phase DFT-optimized structures;  $\omega$ B97XD/SDD(Pt, Zn or Ca)/6-31++g(d,p)(all other atoms).

AIM analysis of hydride-bridged complex **5** shows no considerable binding interaction between Pt and Zn, where no bcp could be located, while the hydride H-atom shows binding to both Pt and Zn centers. Accordingly, NBO analysis reveals strong donation of electron density from the Pt–H  $\sigma$ -bonding orbital to the

vacant  $s$ -orbital on Zn ( $\sigma$ (Pt–H) $\rightarrow$ Zn( $s$ ),  $E^{(2)}$  = 173.59 kcal mol $^{-1}$ ), with only weak backdonation ( $E^{(2)}$  = 5.34 kcal/mol) from the  $d$ -type orbital on Zn to the antibonding  $\sigma^*$ (Pt–H). Therefore, these interactions can be described as donor-acceptor interactions between the Lewis-acidic Zn center and bridging Pt–H fragment. Further supporting the lack of considerable Pt...Zn interactions, only weak donation from the Pt-based  $d$ -orbitals to Zn( $s$ ) was present ( $E^{(2)}$  = 10.71 kcal mol $^{-1}$ ).

In the acetylide complex **11**, the binding interaction of the bridging acetylide with Zn features both  $\sigma$  and  $\pi$ -bonding character via contributions from the donation from the lone pair of the terminal carbon to Zn ( $E^{(2)}$  = 25.00 kcal mol $^{-1}$ ) and weaker  $\pi$ -donation from the bonding  $\pi$ -orbital of the triple C $\equiv$ C bond to the  $s$ -orbital on Zn ( $E^{(2)}$  = 13.95 kcal mol $^{-1}$ ). Backdonation from the occupied  $d$ -orbital on Zn to the antibonding  $\pi^*$  C $\equiv$ C orbital is negligible ( $E^{(2)}$  = 1.47 kcal mol $^{-1}$ ), in contrast to the previously reported Pt/Cu acetylide complex where it is more prominent ( $E^{(2)}$  = 16.14 kcal mol $^{-1}$ ).<sup>[10a]</sup>

NBO analysis of metal-metal interactions in complexes **5** and **11** shows no prominent contribution from the Pt-based  $d$ -orbitals to the  $s$ -orbital on Zn ( $E^{(2)}$  is 12.55 kcal mol $^{-1}$  or less). This parallels the significantly longer Pt...Zn distances (2.7102(7) Å in **5** and 2.9415(8) Å in **11**) in these complexes.

Overall, the computational analyses of metal-metal and metal-ligand binding revealed an interplay between several factors in controlling the extent of metal-metal and metal-bridging ligand interactions. In the case of the Me group, shorter Zn...C distances are present with less coordinately saturated, doubly charged Zn atom, while coordination of triflate to the Zn center leads to elongation of the Zn...C bond with bridging carbon of the methyl group, at the same time leading to greater contribution from Pt...Zn binding interactions. By comparison, replacement of Zn with Ca coordinated to NTF $_2^-$  anions leads to notably weaker or negligible metal-metal and Ca...Me interactions.

## Conclusion

In summary, we report a diverse series of organometallic Pt/Zn complexes featuring variable degrees of Pt...Zn and Zn-bridging ligand (including Me, acetylide or hydride) interactions. In this series, the dimethyl complexes also show synergistic, metal-metal cooperative reactivity in activation of H $_2$ , B–H and Si–H bonds requiring the presence of both Pt and Zn centers in close proximity, different from FLP-type reactivity in monometallic complexes. Such complexes can also be viewed as models of the (retro)transmetalation process between Pt and Zn, demonstrating how the coordination sphere and charge at the Zn center affects relative contribution of Pt...Zn as well as Zn...Me interactions in these complexes. Structure and binding modes found in these complexes resemble intermediates and transition states of the Zn/Pd retrotransmetalation and isomerization relevant to Negishi cross-coupling, previously proposed based on mechanistic and computational studies.

We also compare the binding modes in Pt/Zn complexes with a less conventional combination of Pt with Ca ion, however, in this case only weak or negligible interactions were observed between Pt and Ca centers and Ca and Pt–Me group.

## Acknowledgements

## RESEARCH ARTICLE

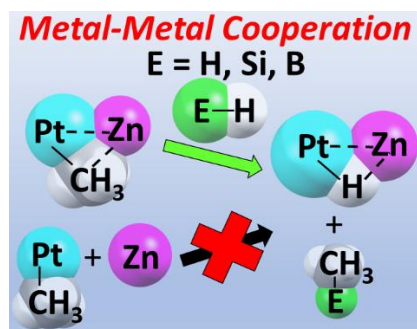
R. R. F. performed crystal structure determination (with exception of complex **6**) within the statements for Kazan Scientific Center of RAS. We thank Instrumental Analysis Section and Engineering Support Section for technical support and Scientific Computing and Data Analysis Section for access to HPC Cluster. The authors acknowledge the Okinawa Institute of Science and Technology Graduate University for funding.

**Keywords:** zinc • platinum • heterobimetallic complexes • metal-metal cooperation • metal-metal interactions

- [1] a) P. Buchwalter, J. Rosé, P. Braunstein, *Chem. Rev.* **2015**, *115*, 28-126; b) D. Das, S. S. Mohapatra, S. Roy, *Chem. Soc. Rev.* **2015**, *44*, 3666-3690; c) D. R. Pye, N. P. Mankad, *Chem. Sci.* **2017**, *8*, 1705-1718; d) K. M. Logan, K. B. Smith, M. K. Brown, *Angew. Chem. Int. Ed.* **2015**, *54*, 5228-5231; ; *Angew. Chem.* **2015**, *127*, 5317-5320; e) W. K. Walker, B. M. Kay, S. A. Michaelis, D. L. Anderson, S. J. Smith, D. H. Ess, D. J. Michaelis, *J. Am. Chem. Soc.* **2015**, *137*, 7371-7378; f) K. Semba, Y. Nakao, *J. Am. Chem. Soc.* **2014**, *136*, 7567-7570.
- [2] M. H. Perez-Temprano, J. A. Casares, P. Espinet, *Chem. - Eur. J.* **2012**, *18*, 1864-1884.
- [3] I. Meana, P. Espinet, A. C. Albéniz, *Organometallics* **2014**, *33*, 1-7.
- [4] R. J. Oeschger, P. Chen, *J. Am. Chem. Soc.* **2017**, *139*, 1069-1072.
- [5] a) R. J. Oeschger, P. Chen, *Organometallics* **2017**, *36*, 1465-1468; b) E. Paenurk, R. Gershoni-Poranne, P. Chen, *Organometallics* **2017**, *36*, 4854-4863.
- [6] a) R. Álvarez, A. R. de Lera, J. M. Aurrecoechea, A. Durana, *Organometallics* **2007**, *26*, 2799-2802; b) B. Fuentes, M. García-Melchor, A. Lledós, F. Maseras, J. A. Casares, G. Ujaque, P. Espinet, *Chem. Eur. J.* **2010**, *16*, 8596-8599; c) J. del Pozo, E. Gioria, J. A. Casares, R. Álvarez, P. Espinet, *Organometallics* **2015**, *34*, 3120-3128; d) J. del Pozo, G. Salas, R. Álvarez, J. A. Casares, P. Espinet, *Organometallics* **2016**, *35*, 3604-3611.
- [7] A. L. Liberman-Martin, D. S. Levine, M. S. Ziegler, R. G. Bergman, T. D. Tilley, *Chem. Commun.* **2016**, *52*, 7039-7042.
- [8] a) F. M. Miloserdov, N. A. Rajabi, J. P. Lowe, M. F. Mahon, S. A. Macgregor, M. K. Whittlesey, *J. Am. Chem. Soc.* **2020**, *142*, 6340-6349; b) I. M. Riddlestone, N. A. Rajabi, J. P. Lowe, M. F. Mahon, S. A. Macgregor, M. K. Whittlesey, *J. Am. Chem. Soc.* **2016**, *138*, 11081-11084.
- [9] a) P. Ingale, K. Knemeyer, P. Preikschas, M. Ye, M. Geske, R. Naumann d'Aloncourt, A. Thomas, F. Rosowski, *Catal. Sci. Technol.* **2021**, *11*, 484-493; b) V. J. Cybulskis, B. C. Bukowski, H.-T. Tseng, J. R. Gallagher, Z. Wu, E. Wegener, A. J. Kropf, B. Ravel, F. H. Ribeiro, J. Greeley, J. T. Miller, *ACS Catal.* **2017**, *7*, 4173-4181; c) C. Chen, M. Sun, Z. Hu, J. Ren, S. Zhang, Z.-Y. Yuan, *Catal. Sci. Technol.* **2019**, *9*, 1979-1988; d) S. W. Han, H. Park, J. Han, J.-C. Kim, J. Lee, C. Jo, R. Ryoo, *ACS Catal.* **2021**, *11*, 9233-9241; e) A. Han, J. Zhang, W. Sun, W. Chen, S. Zhang, Y. Han, Q. Feng, L. Zheng, L. Gu, C. Chen, Q. Peng, D. Wang, Y. Li, *Nat. Commun.* **2019**, *10*, 3787.
- [10] a) S. Deolka, O. Rivada, S. L. Aristizábal, R. R. Fayzullin, S. Pal, K. Nozaki, E. Khaskin, J. R. Khusnutdinova, *Chem. Sci.* **2020**, *11*, 5494-5502; b) O. Rivada-Whealaghan, S. Deolka, R. Govindarajan, E. Khaskin, R. R. Fayzullin, S. Pal, J. R. Khusnutdinova, *Chem. Commun.* **2021**, *57*, 10206-10209; c) O. Rivada-Whealaghan, A. Comas-Vives, R. R. Fayzullin, A. Lledós, J. R. Khusnutdinova, *Chem. Eur. J.* **2020**, *26*, 12168-12179.
- [11] Y. Cai, S. Jiang, L. Dong, X. Xu, *Dalton Trans.* **2022**, *51*, 3817-3827.
- [12] N. Hidalgo, C. Romero-Pérez, C. Maya, I. Fernández, J. Campos, *Organometallics* **2021**, *40*, 1113-1119.
- [13] J. Becica, G. E. Dobreiner, *Org. Biomol. Chem.* **2019**, *17*, 2055-2069.
- [14] J. Bacsa, F. Hanke, S. Hindley, R. Odedra, G. R. Darling, A. C. Jones, A. Steiner, *Angew. Chem. Int. Ed.* **2011**, *50*, 11685-11687; *Angew. Chem.* **2011**, *123*, 11889-11891.
- [15] a) B. Cordero, V. Gomez, A. E. Platero-Prats, M. Reves, J. Echeverria, E. Cremades, F. Barragan, S. Alvarez, *Dalton Trans.* **2008**, 2832-2838; b) P. Pyykkö, M. Atsumi, *Chem. Eur. J.* **2009**, *15*, 186-197.
- [16] M. S. Ziegler, N. A. Torquato, D. S. Levine, A. Nicolay, H. Celik, T. D. Tilley, *Organometallics* **2018**, *37*, 2807-2823.
- [17] J. A. Casares, P. Espinet, B. Fuentes, G. Salas, *J. Am. Chem. Soc.* **2007**, *129*, 3508-3509.
- [18] a) R. van Asselt, C. J. Elsevier, *Organometallics* **1994**, *13*, 1972-1980; b) Q. Liu, Y. Lan, J. Liu, G. Li, Y.-D. Wu, A. Lei, *J. Am. Chem. Soc.* **2009**, *131*, 10201-10210.
- [19] M.-E. Moret, D. Serra, A. Bach, P. Chen, *Angew. Chem., Int. Ed.* **2010**, *49*, 2873-2877; *Angew. Chem.* **2010**, *122*, 2935-2939.
- [20] B. M. Wolf, C. Stuhl, C. Maichle-Mössmer, R. Anwender, *J. Am. Chem. Soc.* **2018**, *140*, 2373-2383.
- [21] a) M. G. Davidson, P. R. Raithby, R. Snaith, D. Stalke, D. S. Wright, *Angew. Chem. Int. Ed.* **1991**, *30*, 1648-1650; *Angew. Chem.* **1991**, *103*, 1696-1697; b) F. G. Baddour, A. S. Hyre, J. L. Guillet, D. Pascual, J. M. Lopez-de-Luzuriaga, T. M. Alam, J. W. Bacon, L. H. Doerrer, *Inorg. Chem.* **2017**, *56*, 452-469; c) I. P. Stolarov, I. A. Yakushev, P. V. Dorovatovskii, Y. V. Zubavichus, V. N. Khrustalev, M. N. Vargaftik, *Mendeleev Commun.* **2018**, *28*, 200-201.
- [22] Deposition Numbers <url href="https://www.ccdc.cam.ac.uk/services/structures?id=doi:10.1002/chem.202201639">2154896 (for **2**), 2154897 (for **3**), 2154898 (for **4**), 2154899 (for **5**), 2169168 (for **6**), 2154900 (for **8**), 2154901 (for **10**), and 2154902 (for **11**) </url> contain(s) the supplementary crystallographic data for this paper. These data are provided free of charge by the joint Cambridge Crystallographic Data Centre and Fachinformationszentrum Karlsruhe <url href="http://www.ccdc.cam.ac.uk/structures">Access Structures service</url>.
- [23] a) Y. Li, C. Hou, J. Jiang, Z. Zhang, C. Zhao, A. J. Page, Z. Ke, *ACS Catal.* **2016**, *6*, 1655-1662; b) Y. Li, J. Liu, X. Huang, L.-B. Qu, C. Zhao, R. Langer, Z. Ke, *Chem. Eur. J.* **2019**, *25*, 13785-13798.
- [24] a) S. J. Hawkes, *J. Chem. Educ.* **1996**, *73*, 516; b) A. P. Latham, Z. M. Heiden, *Dalton Trans.* **2017**, *46*, 5976-5985; c) S. Pal, M. W. Drover, B. O. Patrick, J. A. Love, *Eur. J. Inorg. Chem.* **2016**, *2016*, 2403-2408.
- [25] a) J. R. Fulton, A. W. Holland, D. J. Fox, R. G. Bergman, *Acc. Chem. Res.* **2002**, *35*, 44-56; b) J. E. Bercaw, N. Hazari, J. A. Labinger, P. F. Oblad, *Angew. Chem., Int. Ed.* **2008**, *47*, 9941-9943; *Angew. Chem.* **2008**, *120*, 10089-10091; c) T. J. Williams, A. J. M. Caffyn, N. Hazari, P. F. Oblad, J. A. Labinger, J. E. Bercaw, *J. Am. Chem. Soc.* **2008**, *130*, 2418-2419; d) J. R. Khusnutdinova, N. P. Rath, L. M. Mirica, *J. Am. Chem. Soc.* **2012**, *134*, 2414-2422.
- [26] R. F. W. Bader, *Chem. Rev.* **1991**, *91*, 893-928.
- [27] A. E. Reed, L. A. Curtiss, F. Weinhold, *Chem. Rev.* **1988**, *88*, 899-926.

## RESEARCH ARTICLE

## Entry for the Table of Contents



Pt/Zn and Pt/Ca dimethyl complexes feature various degrees of metal-metal and metal-Me interactions and show Pt/Zn cooperative activation of H<sub>2</sub>, B-H and Si-H bonds, observed only when Zn is in close proximity to Pt, as well as facile protonolysis by water, MeOH and C-H bond of terminal acetylene.

Institute and/or researcher Twitter usernames: @KhusnutdinovaU